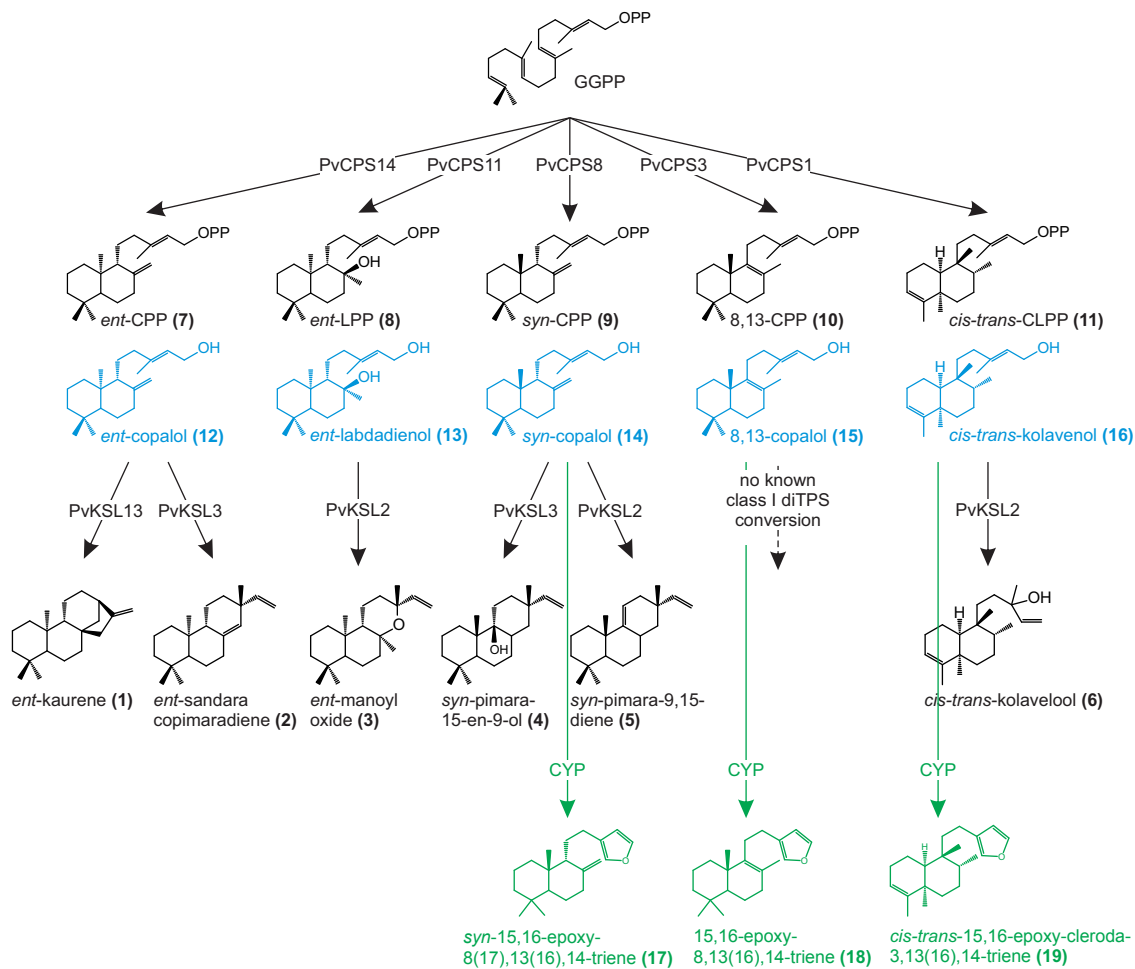
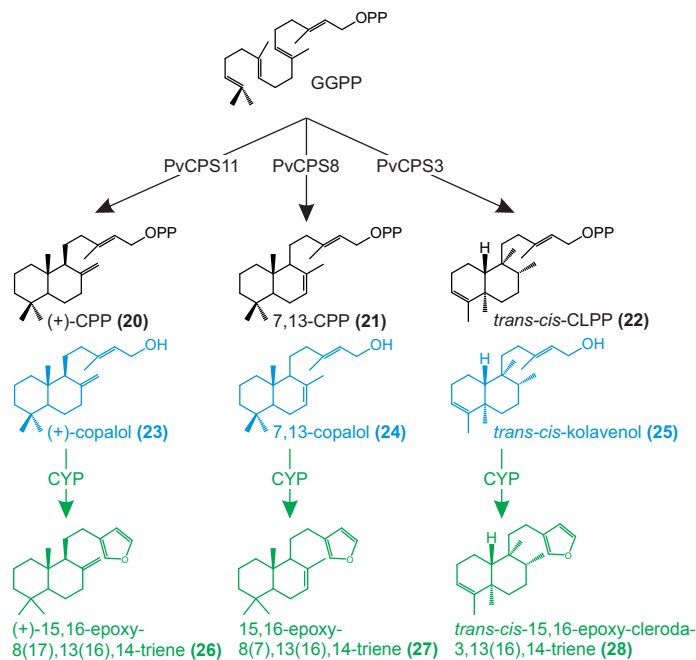


Supplementary Fig. 1: Orthology network of *Panicum virgatum* CYP71Z25-29 paralogs identified in the genomes of *Panicum halli* (v3.1) and *Setaria italica* (v2.2) (<https://phytozome.jgi.doe.gov>). The genes *Pahal.1G276500* and *Pahal.1G276700* derived from the unclustered *P. halli* genome v3.1 are identical to *Pahal.A02218* and *Pahal.A02220* derived from the cluster *P. halli* genome v2.0 used for analysis of genome localization (Fig. 2).

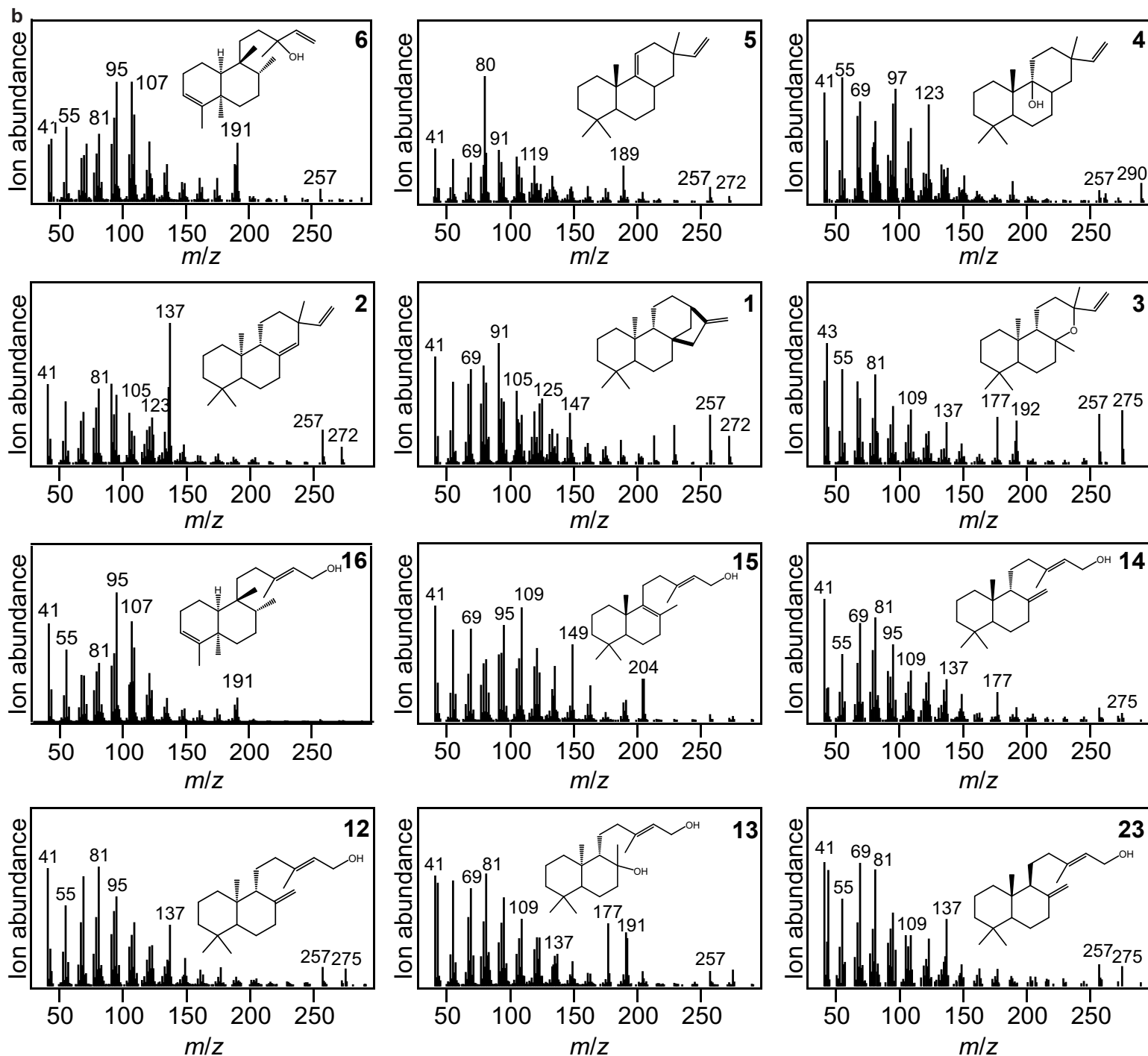
Native *Panicum virgatum* diterpenoid products



Nonnative diterpenoid products



Supplementary Fig. 2. Diterpenoid-metabolic pathways and compounds relevant to this study. Shown are native and nonnative diterpenoid products and corresponding class II and class I diterpene synthases used for the functional analysis of the cytochrome P450 monooxygenases, CYP71Z25-29, in this study. Abbreviations: GGPP, geranylgeranyl pyrophosphate; CPP, copalyl pyrophosphate; LPP, labdadienyl pyrophosphate; CLPP, clerodieryl pyrophosphate; CPS, copalyl diphosphate synthase; KSL, kaurene synthase-like. Blue: alcohol derivatives of corresponding class II diterpene synthase products through the activity of endogenous *E. coli* phosphatases; green: CYP71Z25-29 products from the corresponding class II diterpene synthase alcohol products (12-16, 23-25). Structures of products 26-28 are tentatively assigned based on the structure of the respective class II diterpene synthase products.

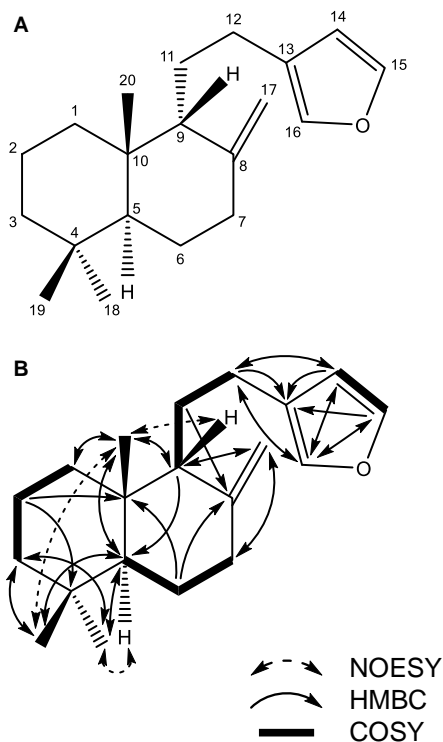


Supplementary Fig. 3. Extracted ion GC-MS mass spectra of relevant products resulting from *E. coli* co-expression of each P450 candidate (CYP71Z25-29) with pairs of diterpene synthases producing core switchgrass diterpene scaffolds. 6, *cis-trans*-kolavelool; 5, *syn*-pimara-9,15-diene; 4, *syn*-pimara-15-ene-9-ol; 2, *ent*-sandracopimaradiene; 1, *ent*-kaurene; 3, *ent*-manoyl oxide; 16, *cis-trans*-kolavenol (i.e. dephosphorylated *cis-trans*-CLPP); 14, *syn*-copalol (i.e. dephosphorylated *syn*-CPP); 12, *ent*-copalol (i.e. dephosphorylated *ent*-CPP); 13, *ent*-labda-8,15-diol (i.e. dephosphorylated *ent*-LPP); 15, 8,13-copalol (i.e. dephosphorylated 8,13-CPP); 23, (+)-copalol (i.e. dephosphorylated (+)-CPP).

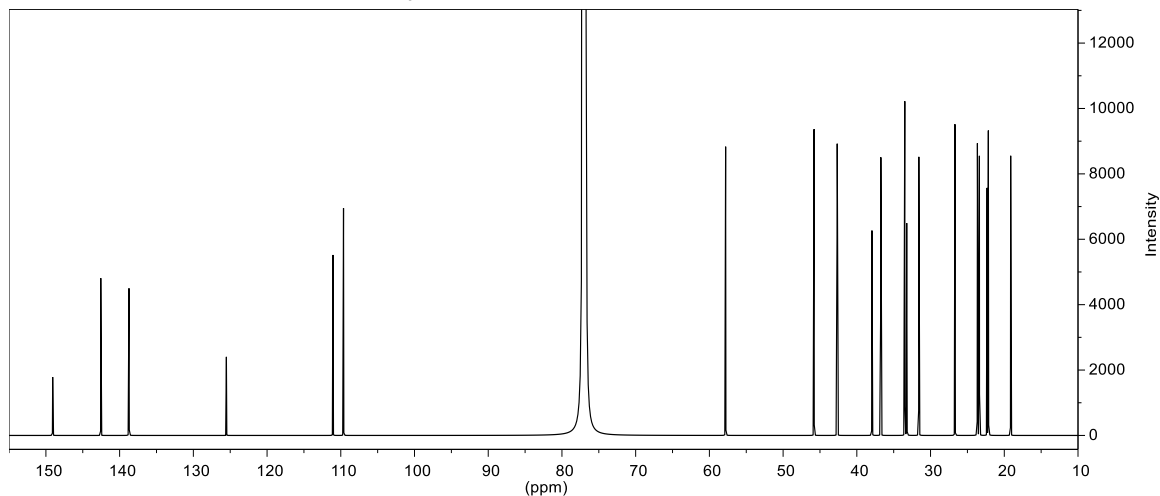
Supplementary Fig 4. NMR analysis of *syn*-15,16-epoxy-8(17),13(16),14-triene (**17**).

Assigned ^{13}C and ^1H chemical shifts for **17** (201 MHz and 800 MHz respectively, CDCl_3 solvent). The structure for **17** was numbered (A) and determined by the selected 2D NMR NOESY, HMBC and COSY correlations (B).

<i>syn</i> -15,16-epoxy-8(17),13(16),14-triene (17)			
Position	δ_{C} (ppm)	δ_{H} (ppm)	J (Hz)
1 a	36.74	1.05 (dq)	12.5, 2.8
b		1.54 (m)	
2 a	19.13	1.43 (dt)	13.3, 3.5
b		1.63 (m)	
3 a	42.66	1.15 (td)	13.3, 3.5
b		1.40 (m)	
4	33.23		
5	45.80	1.30 (m)	
6 a	23.64	1.32 (m)	
b		1.63 (m)	
7 a	31.59	2.10 (m)	
b		2.20 (m)	
8	149.08		
9	57.80	1.60 (m)	
10	37.95		
11 a	26.69	1.58 (m)	
b		1.79 (m)	
12 a	23.37	2.14 (m)	
b		2.33 (ddd)	14.6, 10.6, 4.2
13	125.52		
14	111.07	6.27 (br s)	
15	142.56	7.34 (t)	1.7
16	138.73	7.20 (br s)	
17 a	109.63	4.54 (dd)	2.4, 1.7
b		4.73 (t)	2.4
18	33.49	0.87 (s)	
19	22.16	0.81 (s)	
20	22.33	0.92 (s)	



^{13}C NMR spectrum of **17** (201 MHz, CDCl_3 solvent).

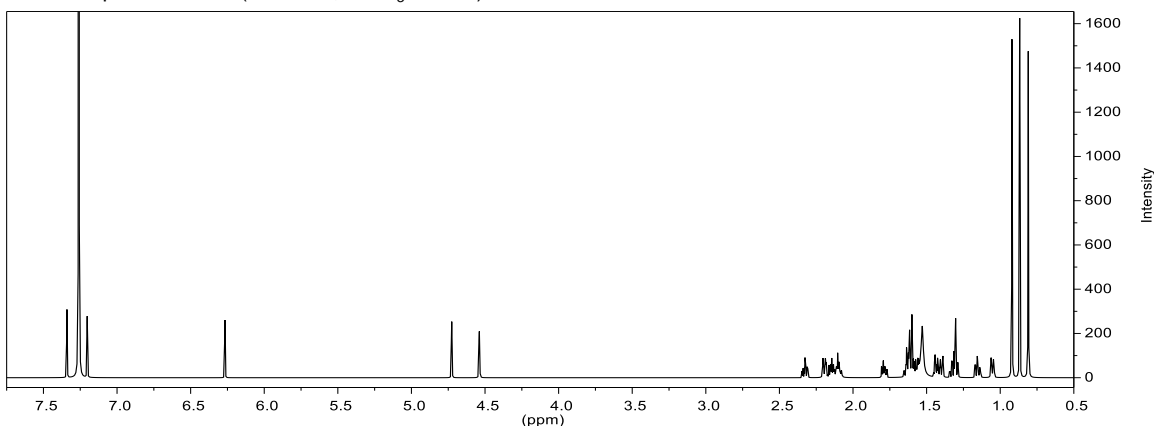


Supplementary Fig. 4, continued

The majority of the bicyclic decalin ¹³C and ¹H NMR chemical shifts of **17** were in agreement (highlighted by *) with the corresponding class II diTPS product of *syn*-copalol (**14**; Yee & Coates (1992) *J. Org. Chem.* 17, 4598-4608).

	(17)	(14)	(17)	(14)
Position	δ_C (ppm)	δ_C (ppm)	δ_H (ppm)	δ_H (ppm)
1 a	36.74*	36.76*	1.05 (dq)	1.05 (br d)
b			1.54 (m)*	1.57*
2 a	19.13*	19.15*	1.43 (dt)*	1.45*
b			1.63 (m)*	1.61*
3 a	42.66*	42.68*	1.15 (td)*	1.17 (td)*
b			1.40 (m)*	1.38*
4	33.23*	33.21*		
5	45.80*	45.78*	1.30 (m)*	1.26*
6 a	23.64*	23.64*	1.32 (m)*	1.30*
b			1.63 (m)*	1.59*
7 a	31.59*	31.56*	2.10 (m)*	2.06*
b			2.20 (m)	2.17 (br d)
8	149.08*	149.20*		
9	57.80*	57.90*	1.60 (m)	1.50
10	37.95*	38.00*		
11 a	26.69	24.46	1.58 (m)	1.47
b			1.79 (m)	1.62
12 a	23.37	38.15	2.14 (m)	1.74
b			2.33 (ddd)	1.90
13	125.52	140.58		
14	111.07	122.94	6.27 (br s)	5.41 (tq)
15	142.56	59.44	7.34 (t)	4.15 (d)
16	138.73	16.52	7.20 (br s)	1.67
17 a	109.63*	109.44*	4.54 (dd)*	4.51 (dd)*
b			4.73 (t)*	4.69 (t)*
18	33.49*	33.49*	0.87 (s)*	0.87*
19	22.16*	22.15*	0.81 (s)*	0.80*
20	22.33*	22.35*	0.92 (s)	0.91 (d)

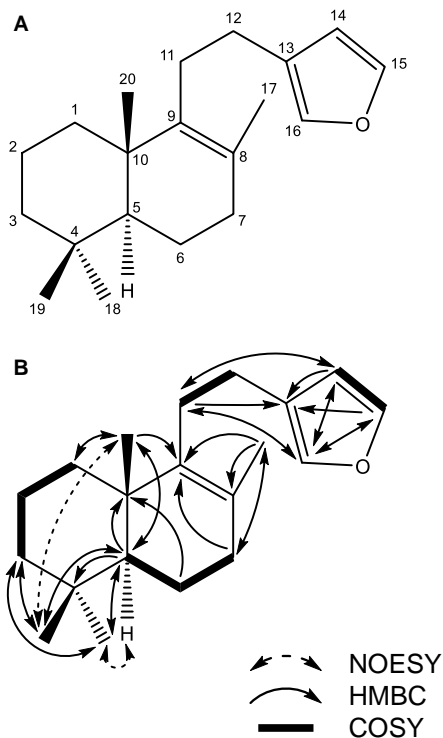
¹H NMR spectrum of **17** (800 MHz, CDCl₃ solvent).



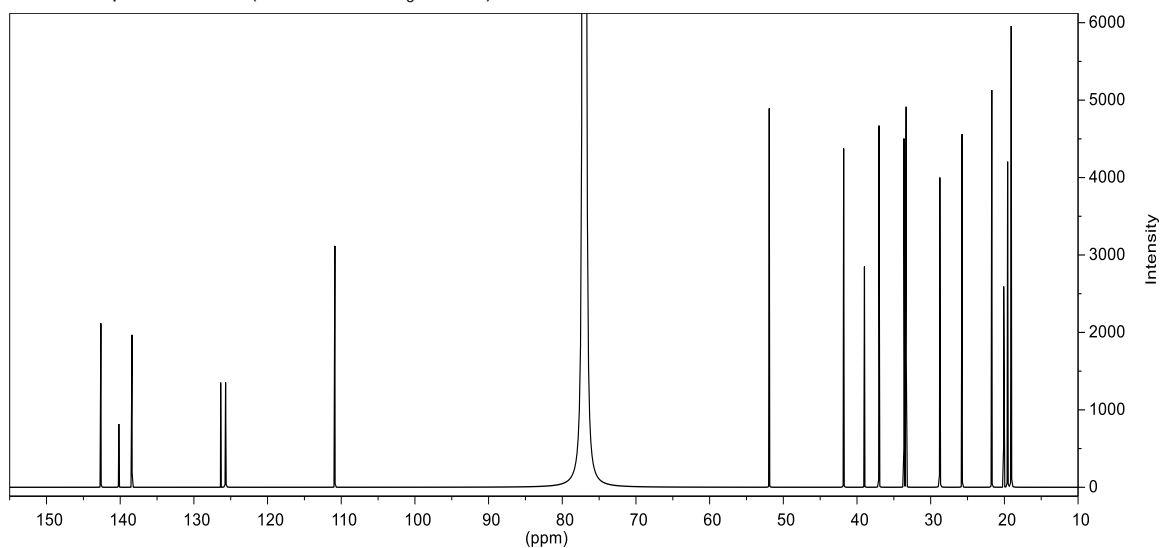
Supplemental Fig 5. NMR analysis of 15,16-epoxy-8,13(16),14-triene (compound **18**).

Assigned ^{13}C and ^1H chemical shifts for **18** (201 MHz and 800 MHz respectively, CDCl_3 solvent). The structure for **18** was numbered (**A**) and determined by the selected 2D NMR NOESY, HMBC and COSY correlations (**B**).

(15,16-epoxy-8,13(16),14-triene (18))			
Position	δ_{C} (ppm)	δ_{H} (ppm)	J (Hz)
1 a	37.02	1.21 (td)	12.9, 3.7
b		1.87 (m)	
2 a	19.07	1.50 (dt)	13.7, 4.0
b		1.62 (m)	
3 a	41.81	1.17 (td)	13.7, 4.0
b		1.42 (m)	
4	33.35		
5	51.91	1.15 (dd)	12.7, 2.0
6 a	19.07	1.42 (m)	
b		1.66 (m)	
7 a	33.63	1.96 (dd)	17.6, 6.3
b		2.06 (m)	
8	126.36		
9	140.19		
10	38.99		
11	25.74	2.45 (dt)	11.3, 6.0
12 a	28.76	2.13 (dt)	11.3, 6.0
b		2.27 (td)	12.5, 12.1, 6.0
13	125.70		
14	110.86	6.30 (br s)	
15	142.62	7.35 (t)	1.7
16	138.40	7.23 (br s)	
17	19.56	1.61 (s)	
18	33.33	0.90 (s)	
19	21.71	0.84 (s)	
20	20.09	0.96 (s)	



^{13}C NMR spectrum of **18** (201 MHz, CDCl_3 solvent).

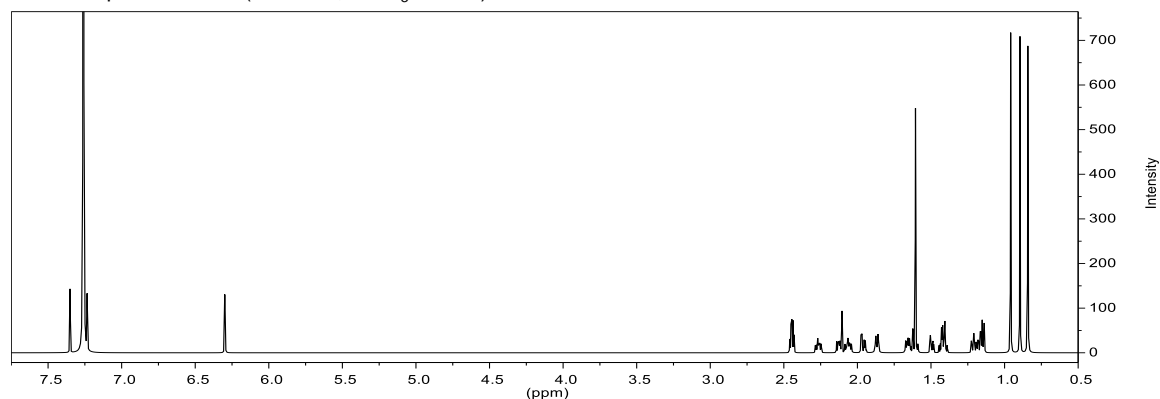


Supplementary Fig. 5, continued

The majority of the bicyclic decalin ^{13}C and ^1H NMR chemical shifts of (**18**) were in agreement (highlighted by *) with the corresponding class II diTPS product of 8,13-copalol (**15**; Pelot *et al.* (2018) *Plant Physiol.* 178(1):54-71).

	(18)	(15)	(18)	(15)
Position	δ_{C} (ppm)	δ_{C} (ppm)	δ_{H} (ppm)	δ_{H} (ppm)
1 a	37.02*	36.97*	1.21 (td)	1.16 (m)
b			1.87 (m)	1.82 (dt)
2 a	19.07*	19.07*	1.50 (dt)*	1.48 (dt)*
b			1.62 (m)*	1.59 (m)*
3 a	41.81*	41.80*	1.17 (td)	1.15 (m)
b			1.42 (m)*	1.41 (m)*
4	33.35*	33.33*		
5	51.91*	51.90*	1.15 (dd)*	1.12 (dd)*
6 a	19.07*	19.07*	1.42 (m)*	1.40 (m)*
b			1.66 (m)*	1.64 (dd)*
7 a	33.63*	33.64*	1.96 (dd)*	1.94 (dd)*
b			2.06 (m)*	2.04 (m)*
8	126.36*	126.04*		
9	140.19*	140.13*		
10	38.99*	39.05*		
11 a	25.74	26.77	2.45 (dt)	1.98 (td)
b				2.12 (td)
12 a	28.76	40.16	2.13 (dt)	2.05 (m)
b			2.27 (td)	
13	125.70	140.79		
14	110.86	122.60	6.30 (br s)	5.43 (tq)
15	142.62	59.44	7.35 (t)	4.16 (d)
16	138.40	16.36	7.23 (br s)	1.71 (s)
17	19.56*	19.51*	1.61 (s)*	1.58 (s)*
18	33.33*	33.32*	0.90 (s)*	0.88 (s)*
19	21.71*	21.70*	0.84 (s)*	0.83 (s)*
20	20.09*	20.09*	0.96 (s)*	0.94 (s)*

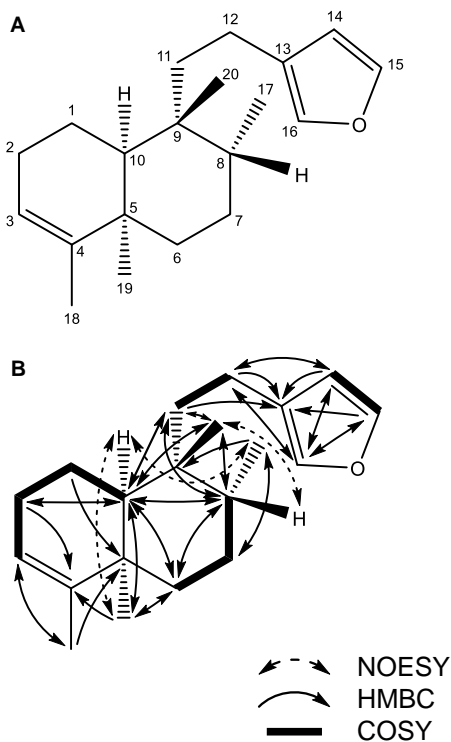
^1H NMR spectrum of **18** (800 MHz, CDCl_3 solvent).



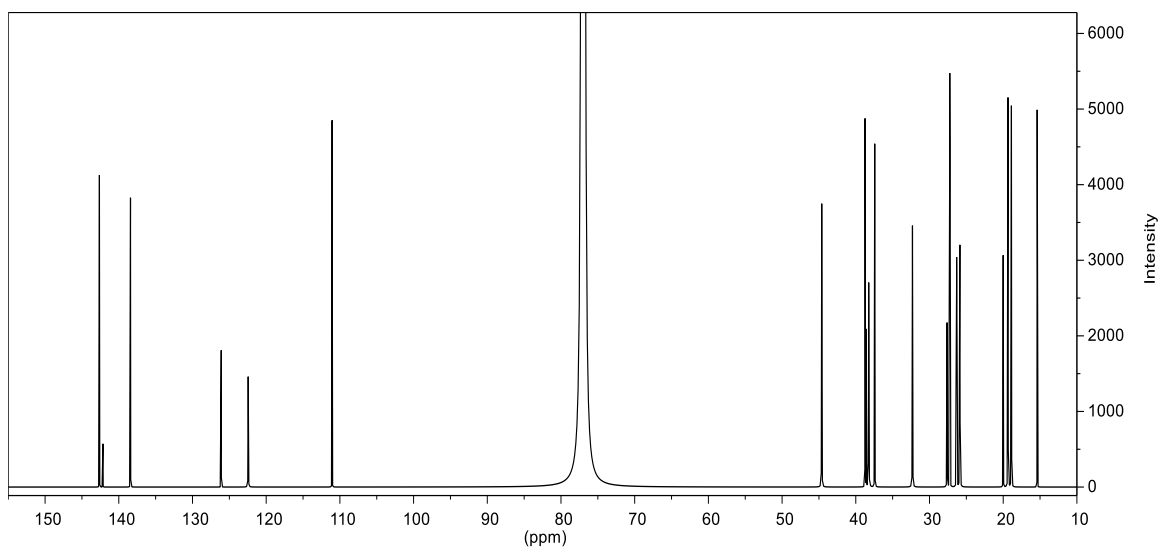
Supplementary Fig. 6. NMR analysis of *cis-trans*-15,16-epoxy-cleroda-3,13(16),14-triene (**19**).

Assigned ^{13}C and ^1H chemical shifts for **19** (201 MHz and 800 MHz respectively, CDCl_3 solvent). The structure for **19** was numbered (A) and determined by the selected 2D NMR NOESY, HMBC and COSY correlations (B).

<i>cis-trans</i> -15,16-epoxy-cleroda-3,13(16),14-triene (19)			
Position	δ_{C} (ppm)	δ_{H} (ppm)	J (Hz)
1 a	20.00	1.62 (m)	
b		1.82 (m)	
2 a	25.88	1.94 (m)	
b		2.01 (m)	
3	122.44	5.35 (br s)	
4	142.15		
5	38.74		
6 a	32.31	1.50 (m)	
b		1.63 (m)	
7 a	27.25	1.36 (m)	
b		1.43 (m)	
8	37.43	1.60 (m)	
9	38.61		
10	44.62	1.50 (m)	
11 a	38.25	1.39 (td)	13.6, 4.2
b		1.98 (td)	13.6, 4.7
12 a	18.88	2.33 (td)	13.6, 4.2
b		2.45 (td)	13.6, 4.7
13	126.10		
14	111.06	6.28 (br s)	
15	142.63	7.35 (t)	1.7
16	138.41	7.21 (br s)	
17	15.39	0.88 (d)	7.0
18	19.35	1.65 (q)	1.8
19	27.62	1.18 (s)	
20	26.31	1.08 (s)	



^{13}C NMR spectrum of **19** (201 MHz, CDCl_3 solvent).

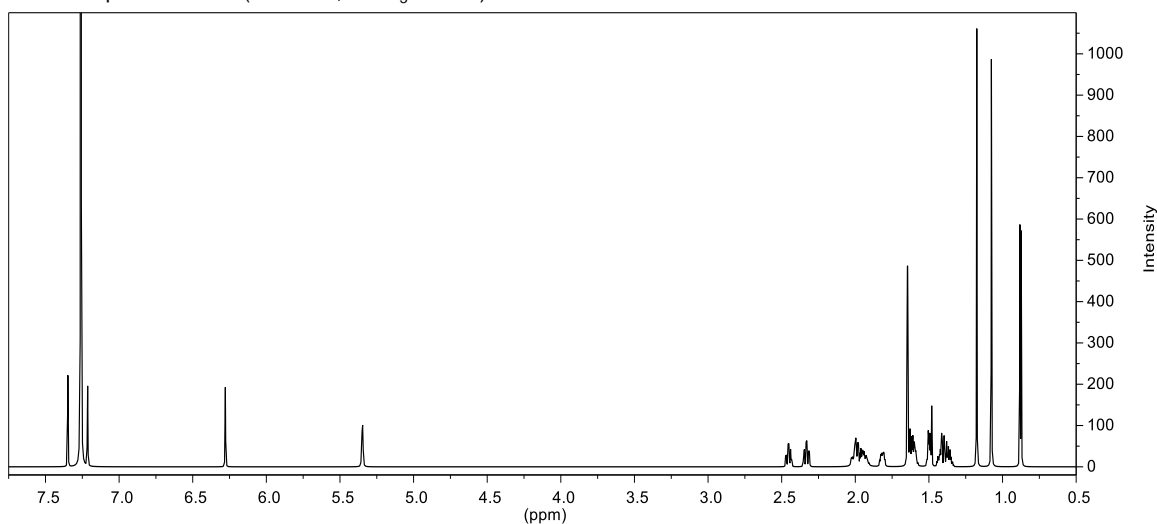


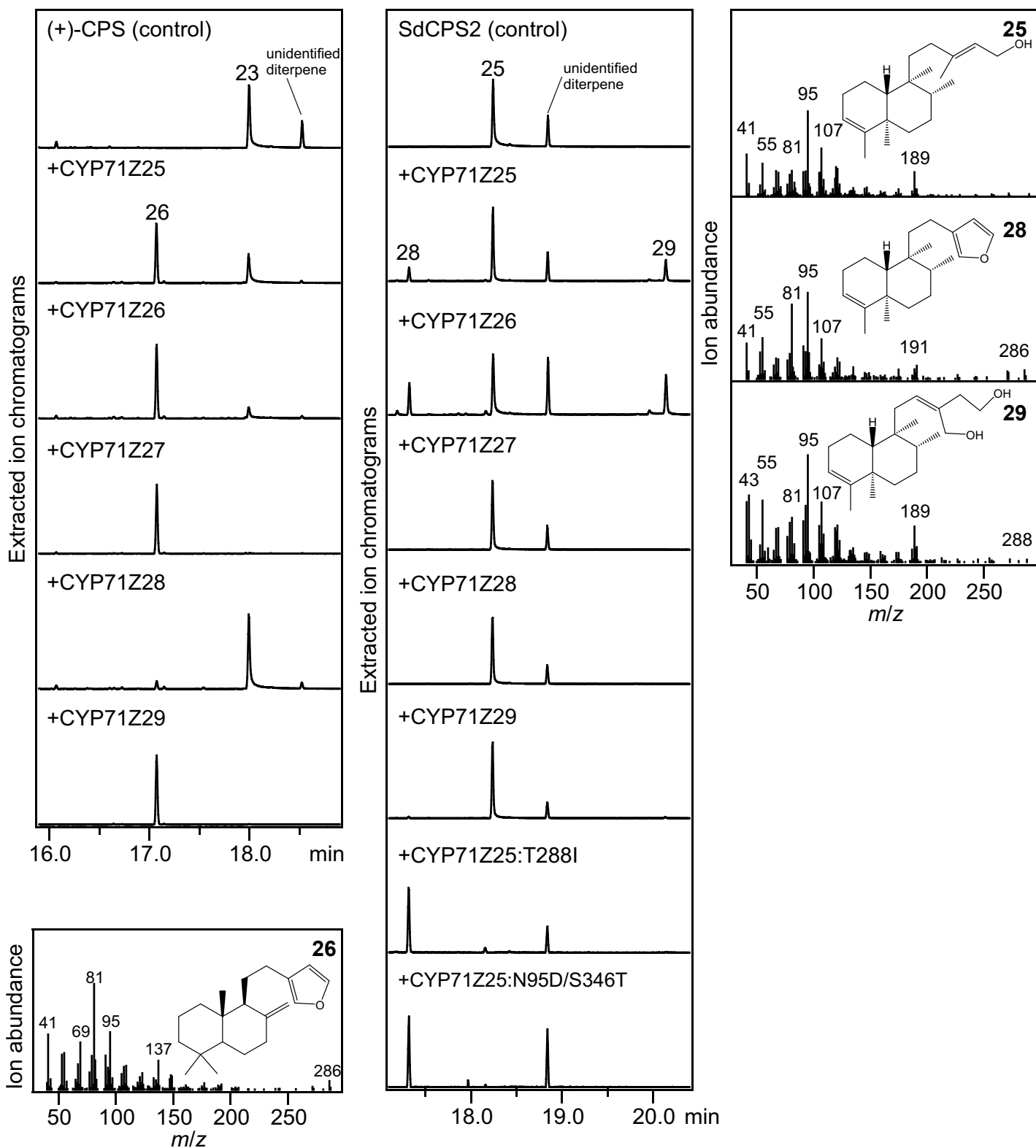
Supplementary Fig. 6, continued

The majority of the bicyclic decalin ¹³C and ¹H NMR chemical shifts of **19** were in agreement (highlighted by *) with the corresponding class II diTPS product of *cis-trans*-kolavenol (**16**; Pelot *et al.* (2018) *Plant Physiol.* 178(1):54-71).

	(19)	(16)	(19)	(16)
Position	δ_c (ppm)	δ_c (ppm)	δ_H (ppm)	δ_H (ppm)
1 a	20.00*	20.01*	1.62 (m)*	1.60 (m)*
b			1.82 (m)*	1.80 (m)*
2 a	25.88*	25.87*	1.94 (m)*	1.93 (m)*
b			2.01 (m)*	1.98 (m)*
3	122.44*	122.41*	5.35 (br s)*	5.34 (br s)*
4	142.15*	142.16*		
5	38.74*	38.77*		
6 a	32.31*	32.32*	1.50 (m)*	1.48 (m)*
b			1.63 (m)*	1.61 (m)*
7 a	27.25*	27.25*	1.36 (m)*	1.35 (m)*
b			1.43 (m)*	1.41 (m)*
8	37.43*	37.50*	1.60 (m)*	1.56 (m)*
9	38.61*	38.59*		
10	44.62*	44.63*	1.50 (m)	1.43 (dd)
11 a	38.25	36.03	1.39 (td)	1.23 (td)
b			1.98 (td)	1.83 (td)
12 a	18.88	33.42	2.33 (td)	1.91 (td)
b			2.45 (td)	2.05 (td)
13	126.10	141.35		
14	111.06	122.67	6.28 (br s)	5.42 (tq)
15	142.63	59.48	7.35 (t)	4.16 (d)
16	138.41	16.60	7.21 (br s)	1.70 (br s)
17	15.39*	15.38*	0.88 (d)*	0.86 (d)*
18	19.35*	19.35*	1.65 (q)*	1.64 (q)*
19	27.62*	27.71*	1.18 (s)*	1.15 (s)*
20	26.31*	26.41*	1.08 (s)*	1.02 (s)*

¹H NMR spectrum of **19** (800 MHz, CDCl₃ solvent).



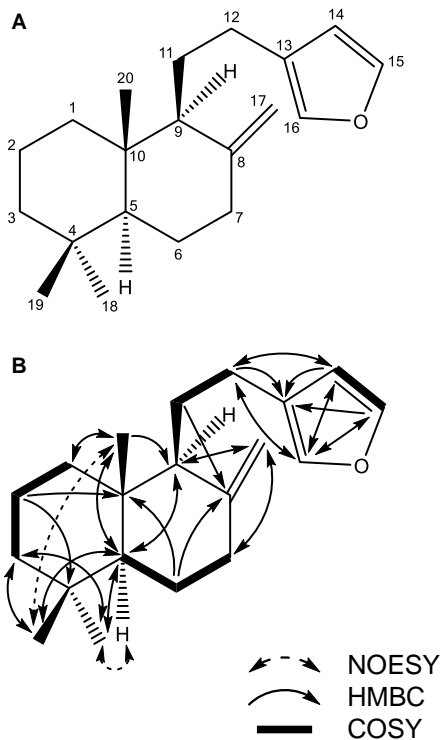


Supplementary Fig. 7. Functional characterization of switchgrass P450s. Individually scaled extracted ion GC-MS chromatograms and corresponding mass spectra of reaction products resulting from *E. coli* co-expression assays of the individual constructs of CYP71Z25 and selected P450 variants with class II diTPSs producing (+)-copalol (i.e. dephosphorylated (+)-CPP) or *trans-cis*-kolavenol (i.e. dephosphorylated *trans-cis*-CLPP produced by *Salvia divinorum* CPS2). 23, (+)-copalol (i.e. dephosphorylated (+)-CPP); 25, *trans-cis*-kolavenol (i.e. dephosphorylated *trans-cis*-CLPP); 26, (+)-15,16-epoxy-8(17),13(16),14-triene; 29, *trans-cis*-cleroda-3,12-dien-15,16-diol; 28, predicted furanoditerpenoid derivative of 25. Structures of the furanoditerpenoid product 28 and dihydroxyl product 29 were assigned on the basis of the respective substrate structures.

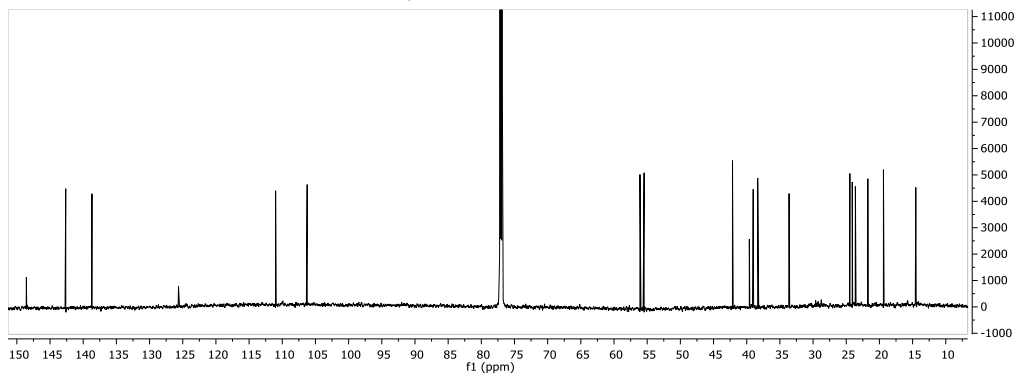
Supplementary Fig. 8. NMR analysis of (+)-15,16-epoxy-8(17),13(16),14-triene (**26**).

Assigned ^{13}C and ^1H chemical shifts for **26** (201 MHz and 800 MHz respectively, CDCl_3 solvent). The structure for **26** was numbered (A) and determined by the selected NMR NOESY, HMBC and COSY correlations (B).

(+)-15,16-epoxy-8(17),13(16),14-triene (26)			
Position	δ_{C} (ppm)	δ_{H} (ppm)	J (Hz)
1 a	39.02	0.97 (td)	13.0, 3.9
b		1.74 (m)	
2 a	19.39	1.47 (m)	
b		1.56 (m)	
3 a	42.66	1.16 (td)	13.4, 4.1
b		1.39 (m)	
4	33.59		
5	55.47	1.07 (dd)	12.6, 2.8
6 a	24.45	1.33 (m)	
b		1.74 (m)	
7 a	38.35	1.98 (td)	13.0, 5.1
b		2.40 (m)	
8	148.57		
9	56.09	1.64 (m)	
10	39.61		
11 a	24.09	1.61 (m)	
b		1.76 (m)	
12 a	23.62	2.23 (m)	
b		2.55 (m)	
13	125.64		
14	111.00	6.26 (m)	
15	142.63	7.35 (t)	1.6
16	138.68	7.19 (m)	
17 a	106.25	4.56 (m)	
b		4.86 (m)	
18	33.62	0.86 (s)	
19	21.74	0.80 (s)	
20	14.52	0.68 (s)	



^{13}C NMR spectrum of **26** (201 MHz, CDCl_3 solvent).



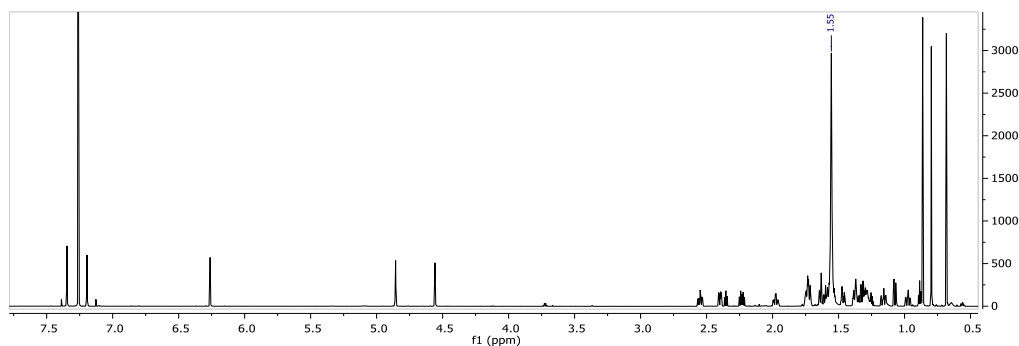
Supplementary Fig. 8, continued

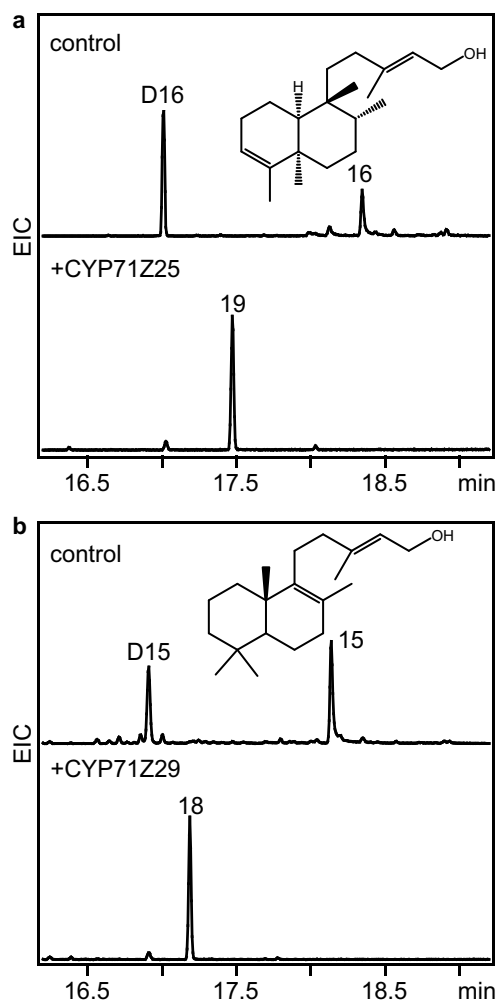
The majority of the bicyclic decalin ^{13}C and ^1H NMR chemical shifts of **26** were in agreement (highlighted by *) with the corresponding class II diTPS product of (+)-copalol (**23**; Yee & Coates (1992) *J. Org. Chem.* 17, 4598-4608).

H_2O
peak

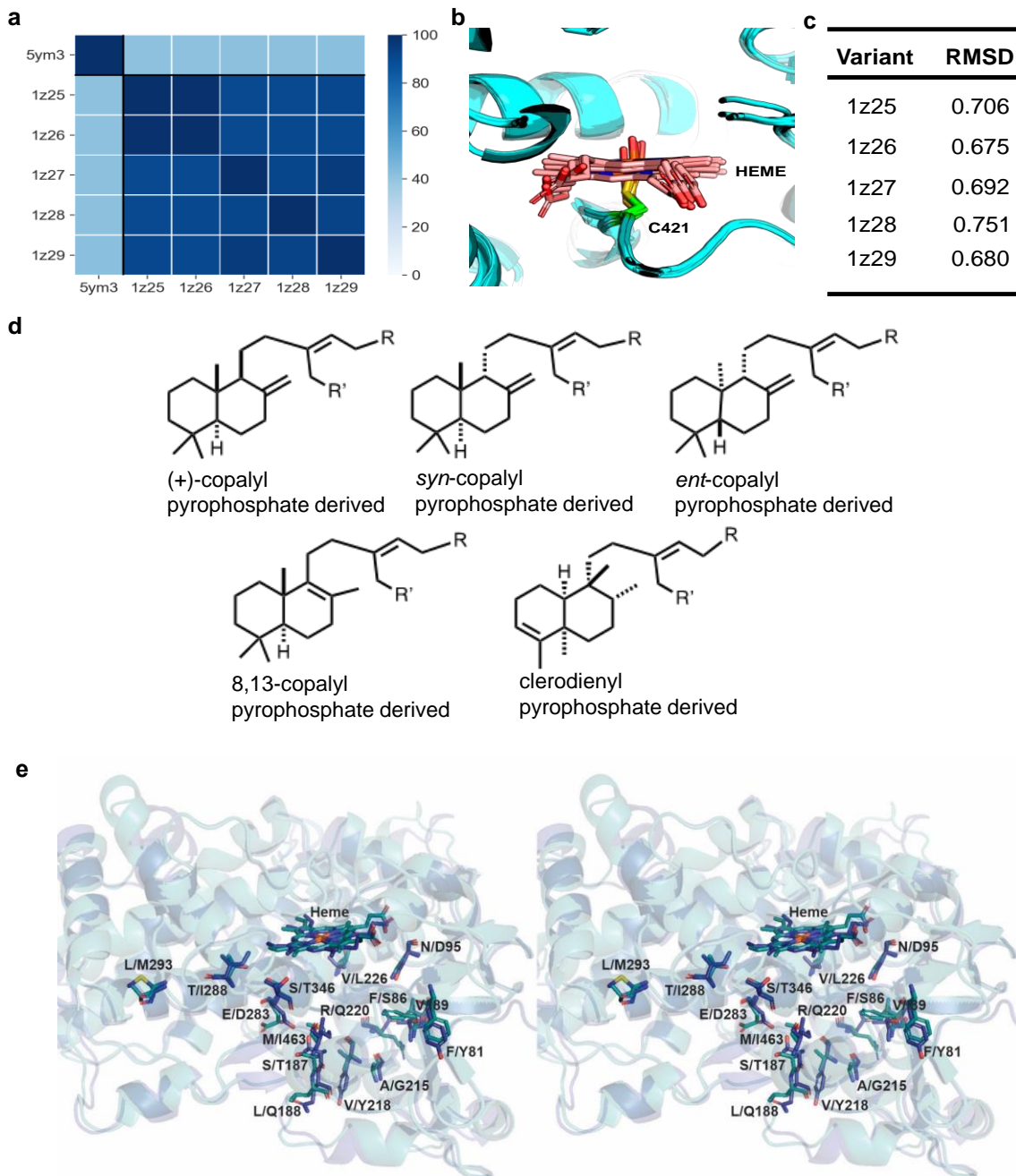
	(26)	(23)	(26)	(23)
Position	δ_{C} (ppm)	δ_{C} (ppm)	δ_{H} (ppm)	δ_{H} (ppm)
1 a	39.02*	39.19*	0.97 (td) *	0.99 (td) *
b			1.74 (m) *	1.72*
2 a	19.39	21.89	1.47 (m)	1.39*
b			1.56 (m) *	1.57*
3 a	42.66*	42.27*	1.16 (td) *	1.16 (td)*
b			1.39 (m) *	1.37*
4	33.59*	33.71*		
5	55.47*	55.63*	1.07 (dd) *	1.07 (dd)*
6 a	24.45*	24.56*	1.33 (m) *	1.30*
b			1.74 (m) *	1.70*
7 a	38.35*	38.47*	1.98 (td) *	1.96 (td)*
b			2.40 (m) *	2.38*
8	148.57*	148.74*		
9	56.09*	56.40*	1.64 (m)	1.54
10	39.61*	39.77*		
11 a	24.09	19.52	1.61 (m)	1.45
b			1.76 (m)	1.60
12 a	23.62	38.55	2.23 (m)	1.79
b			2.55 (m)	2.15
13	125.64	140.78		
14	111.00	123.05	6.26 (m)	5.38 (tq)
15	142.63	59.54	7.35 (t)	4.15 (d)
16	138.68	16.49	7.19 (m)	1.65
17 a	106.25*	106.38*	4.56 (m) *	4.50 (br d)*
b			4.86 (m) *	4.82 (app q)*
18	33.62*	33.75*	0.86 (s) *	0.86*
19	21.74*	21.86*	0.80 (s) *	0.79*
20	14.52*	14.62*	0.68 (s) *	0.67*

^1H NMR spectrum of **26** (800 MHz, CDCl_3 solvent). (Note peak 1.55 represents probably water impurity)

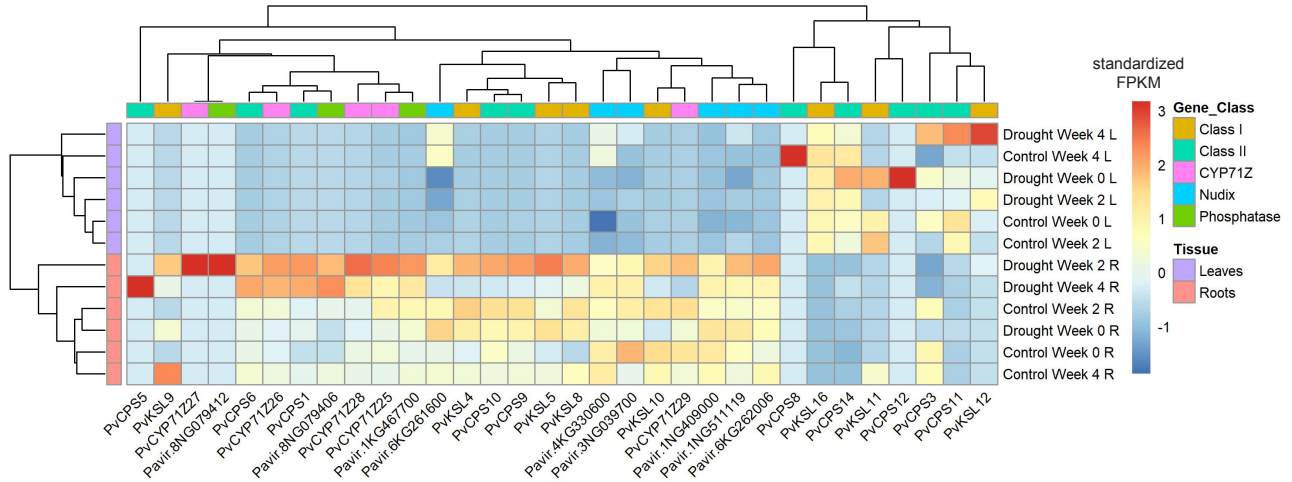




Supplementary Figure 9. Substrate-specificity of switchgrass CYP71Z25-29. Individually scaled extracted ion GC-MS chromatograms of enzyme products resulting from *E. coli* expression of CYP71Z25 or CYP71Z29 with purified diterpenoid alcohol substrates added to the culture. **(a)** *E. coli* expression of CYP71Z25 with purified 16 (dephosphorylated 11) added as a substrate. Compound D16 is a derivative of 16 presumably through isomerization during the *E. coli* expression. **(b)** *E. coli* expression of CYP71Z29 with purified 15 (dephosphorylated 10) added as a substrate. Compound D15 is a putative derivative of 15 presumably through isomerization during the *E. coli* expression.



Supplementary Fig. 10: Structural analysis of CYP71Z25-29. **(a)** Heatmap of pairwise identity between the template (*Salvia miltiorrhiza* CYP76AH155; PDB-ID 5YM3) and CYP71Z25-29, and between each P450 variant. **(b)** Overlay of each CYP71Z25-29 models active site (teal, template gray) with heme (pink) and residue C421 (green). **(c)** RMSD (root-mean-square deviation) values of the generated structural models of CYP71Z25-29 as compared to the template **(d)** Structures of the three possible substitution arrangements (15-hydroxy, R=OH, R'=H; 15-pyrophosphate, R=OPP, R'=H; 15,16-dihydroxy, R=OH, R'=OH for all five P450 substrates investigated via ligand docking in this study. **(e)** Stereo view representation of a structural overlay of homology models of CYP71Z25 (teal) and CYP71Z29 (blue), illustrating active site residues targeted for site-directed mutagenesis in this study.



Supplemental Figure 11. Hierarchical cluster analysis of the gene expression of a predicted dolichyldiphosphatase (*Pavir.1KG467700*), two putative phosphoserine phosphatases (*Pavir.8NG079406*, *Pavir.8NG079412*) and putative Nudix hydrolase genes (*Pavir.6KG261600*, *Pavir.4KG330600*, *Pavir.3NG039700*, *Pavir.1NG409000*, *Pavir.1NG511119*, *Pavir.6KG262006*) as compared to select diTPS and CYP71Z25-29 gene expression profiles from drought stressed switchgrass tissues. Samples were collected before starting treatment (W0), two weeks (W2), and four weeks (W4) of drought stress treatment. L=leaves, R=roots, Drought stressed=D, well-watered=C.